J|A|C|S COMMUNICATIONS

Published on Web 12/03/2010

A Remarkably Bent Diiron(III)-μ-Hydroxo Bisporphyrin: Unusual Stabilization of Two Spin States of Iron in a Single Molecular Framework

Sudip Kumar Ghosh and Sankar Prasad Rath*

Department of Chemistry, Indian Institute of Technology Kanpur, Kanpur 208016, India

Received August 24, 2010; E-mail: sprath@iitk.ac.in

Abstract: A novel diiron(III) bisporphyrin bridged by a hydroxo group between two cofacial Fe centers is reported. X-ray structural characterization revealed the remarkably bent μ-hydroxobis[Fe(III) porphyrin] with the smallest known Fe−O(H)−Fe angle [142.5(2)°] reported to date in an iron porphyrin. The close approach of the two rings in the molecule results in an unequal core deformation, and as a result, the geometrical parameters (such as the Fe−N_p, Fe−O and Fe···Ct_p distances) are all different for the two Fe(III) centers, leading for the first time to a natural way of stabilizing two different spins of iron in a single molecular framework with complete retention of their own spectroscopic identities in both the solid state and solution. The strong antiferromagnetic coupling between the two Fe(III) centers in the μ-oxo dimer ($-J$ = 126.6 cm^{-1}) is attenuated to only 4.5 cm^{-1} simply by protonation to give the μ-hydroxo complex.

Oxo- or hydroxo-bridged diiron active centers are structural motifs commonly found among proteins involved in O_2 metabolism, such as hemerythrin, the hydroxylase component of methane monooxygenase (MMOH), the R2 subunit of class I ribonucleotide reductases (RNRR2), and fatty acid desaturases.[1−4] The transformation of an oxo bridge into a hydroxo bridge is an obligatory or proposed step in the reaction pathways of a great variety of iron and copper redox enzymes.[1] Structurally, Fe−O−Fe units tend toward linearity because of π-bonding and steric effects. Upon protonation, the Fe−O(H)−Fe unit becomes bent, resulting in two Fe(III) centers that are indistinguishable.[2a,b] Here we report a novel example of a diiron(III) bisporphyrin bridged by a single hydroxo group between the two Fe centers in which the Fe−O(H)−Fe angle is the smallest ever reported for an iron porphyrin and also in which two different spins of Fe have, for the first time, been stabilized in a single molecular framework, although the two cores contain exactly the same chemical entity.

Shaking a dichloromethane solution of **1** with 3 M NaOH affords the remarkably bent μ-oxobis[Fe(III) porphyrin] **2**,[4] which upon addition of HI/I_2 changes color immediately from green to red as a result of the formation of μ-hydroxo complex **3** (Scheme 1). The molecule was then isolated as a solid in high yield and structurally characterized (see the Supporting Information for details). The UV−vis spectrum of **3** showed a large blue shift in the Soret band with λ_{max} at 380 nm in CH_2Cl_2 (Figure S1 in the Supporting Information), while the electrospray ionization mass spectrometry (ESI-MS) spectrum (positive-ion mode) showed an intense peak at *m*/*z* 1219.6011 for $[\mathbf{3}]^+$ (Figure S2).

Dark-purple crystals[5] of **3** were grown by slow diffusion of *n*-hexane into a THF solution of the complex at room temperature. Figure 1 and Figure S3 show the X-ray structure of the molecule and the packing diagram, respectively. The proton of the hydroxo bridge was directly located in the difference Fourier maps with an O−H distance of 0.80(6) Å and was also found to be engaged in H-bonding interactions with the oxygen of THF [O1···O1S = 2.628(5)Å] present as a solvent molecule of crystallization. To date there have been only three structural reports of two iron porphyrins bridged by a single hydroxo group.[2a,b]

Scheme 1

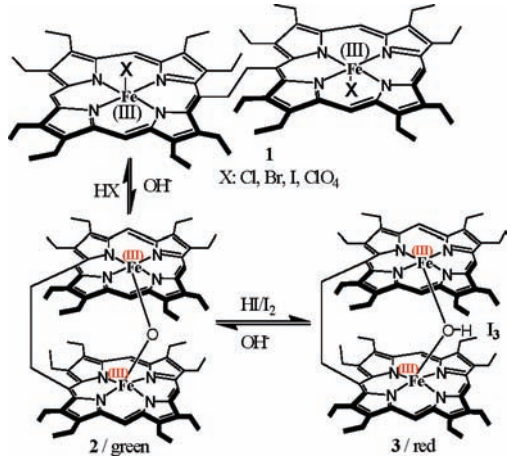

We recently reported that μ-oxobis[Fe(III) porphyrin] **2** exhibits the smallest Fe−O−Fe angle (147.9°).[4] Upon protonation, the Fe−O(H)−Fe unit becomes further bent by 5.4°, resulting in the smallest Fe−O(H)−Fe angle (142.5°) reported[2] for a porphyrinic system. Table 1 compares the salient structural features of μ-hydroxo complex **3** with those of the corresponding μ-oxo dimer **2**.

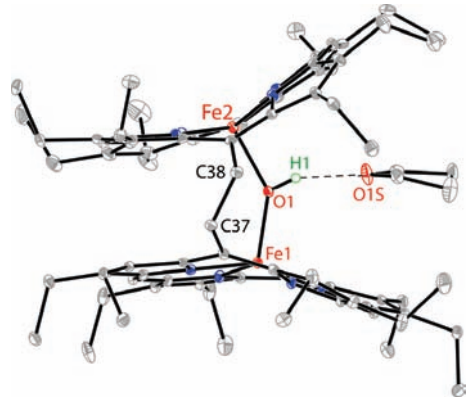

Figure 1. Perspective view of **3** (without I_3 counteranion) showing 50% thermal contours for all non-hydrogen atoms at 100 K (all of the hydrogens except for the μ-hydroxo proton have been omitted for clarity). Selected bond distances (Å) and angle (deg): Fe1−O1, 1.897(3); Fe1−N1, 2.055(4); Fe1−N2, 2.054(4); Fe1−N3, 2.054(4); Fe1−N4, 2.041(4); Fe2−O1, 1.934(3); Fe2−N101, 2.002(4); Fe2−N102, 2.015(4); Fe2−N103, 1.994(4); Fe2−N104, 2.016(4); C37−C38, 1.553(7); O1−H1, 0.80(6); Fe1−O1−Fe2, 142.5(2).

Table 1. Selected Geometrical Parameters

	2		3	
	core I	core II	core I	core II
Fe−O (Å)	1.779(2)	1.768(2)	1.897(3)	1.934(3)
Fe−N_p (Å)[a]	2.068(3)	2.072(3)	2.051(3)	2.007(3)
Fe−O−Fe (deg)	147.9(1)		142.5(2)	
Δ_{24}^{Fe} (Å)[b]	0.55	0.60	0.55	0.48
Fe···Fe (Å)	3.409(1)		3.627(1)	
Δ_{24} (Å)[c]	0.20	0.21	0.21	0.31
twist angle (deg)[d]	16.1		12.9	

[a] Average value. [b] Displacement of iron from the least-squares plane of the $C_{20}N_4$ pophyrinato core. [c] Average displacement of atoms from the least-squares plane of the $C_{20}N_4$ pophyrinato core. [d] Average of the four N−Fe−Fe′−N′ dihedral angles.

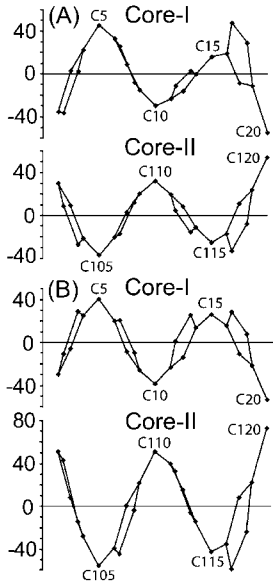

Figure 2. Atom deviations (in units of 0.01 Å) from the least-squares plane of the $C_{20}N_4$ porphyrinato core in (A) **2** and (B) **3**. The horizontal axis represents the atom number in the macrocycle (the numbering scheme is shown in Figure S4), showing the bond connectivity between atoms.

As can be seen, the most remarkable features of **3** are the very different geometrical parameters for Fe in the two cores. The Fe−O bonds undergo unequal elongation from nearly equal distances of 1.779(2) and 1.768(2) Å in **2** to 1.897(3) and 1.934(3) Å in μ-hydroxo complex **3**. The Fe−N distances in the two cores are also very different: the average distances are 2.051 Å in core I and 2.007 Å in core II. The out-of-plane displacement of Fe from the least-squares plane of the $C_{20}N_4$ pophyrinato core (Fe···Ct_p) in **3** is the same as that in **2** for core I (0.55 Å), but the value for core II is contracted from 0.60 to 0.48 Å. All of the structural features for core I are characteristic of a nearly high-spin ($S = {}^5/_2$) nature of Fe, while the structural parameters for core II are all in the direction expected for an admixture of a fairly small amount of $S = {}^5/_2$ character into a predominantly $S = {}^3/_2$ spin state.[6] The close approach of the two rings in **3** leads to an unequal core deformation (core II is more distorted than core I), which can be seen in the out-of-plane displacement plots of the porphyrin core atoms (Figure 2 and Figure S4) and is responsible for the unusual stabilization of two different spins of iron in the same molecule.

The presence of two different spins of Fe in **3** is also reflected in the solid-state Mössbauer spectra (Figure 3). **2** shows small quadrupole splitting [δ (ΔEq): 0.28 (0.61) mm/s] at 295 K that is characteristic of the high-spin nature of Fe(III), while **3** exhibits two quadrupole-split doublets [δ (ΔEq): 0.28 (1.16) and 0.29 (2.35)

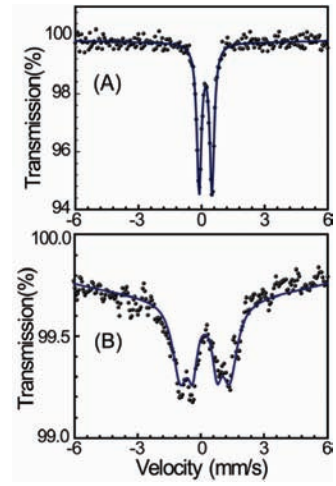

Figure 3. Mössbauer spectra at 295 K for (A) **2** and (B) **3**.

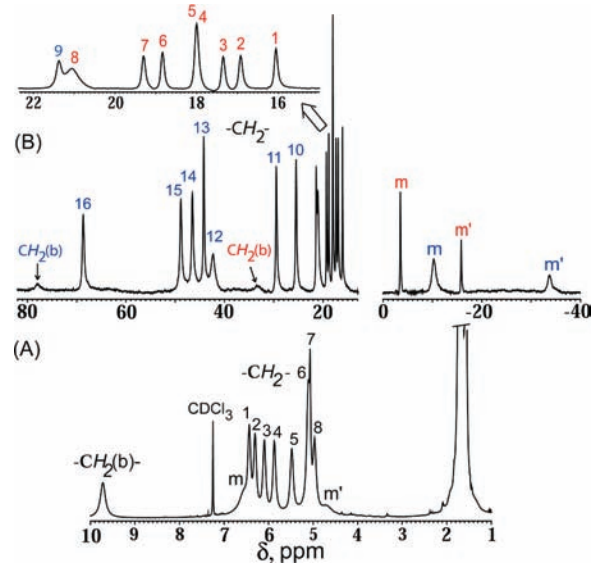

Figure 4. ^{1}H NMR spectra in $CDCl_3$ at 295 K for (A) **2** and (B) **3**.

mm/s] corresponding to two inequivalent Fe(III) centers, one being high-spin (with minor contribution of $S = {}^3/_2$) and the other having admixed intermediate spins, as also observed in the X-ray structure (see above). The solid- and solution-phase electron paramagnetic resonance spectra at 120 K were too broad to be characteristic for the spin states.

The solid-state structure was also preserved in solution, as reflected in the ESI-MS analysis (Figure S2) and ^{1}H NMR spectra in $CDCl_3$ (Figure 4). For the μ-oxo dimer **2**, eight broad methylene proton resonances and two meso signals in a 1:2 intensity ratio within the 4−7 ppm region were observed (trace A) as a result of strong antiferromagnetic coupling between the two equivalent high-spin Fe(III) centers.[4a] However, 16 methylene and four meso signals (trace B) were generated just upon protonation of the oxo group to form the μ-hydroxo dimer **3**, again confirming the presence of two different Fe(III) centers within the same molecular framework, which can also be seen by the two distinct sets of signals. In one set, eight broad methylene signals spanning the range from 68.8 to 21.2 ppm (average 41.2 ppm) along with two broad meso proton signals at −10.3 and −35.5 ppm in a 2:1 intensity ratio were observed for core I. In the other set, eight sharp methylene peaks in the relatively narrow region from 19.9 to 16.1 ppm (average 18.1 ppm) and two sharp meso resonances at −3.5 and −15.9 ppm

in a 2:1 intensity ratio appeared for core II. Earlier, it was observed that $-CH_2$ proton signals of high-spin complex **1** were shifted downfield to approximately +40 ppm while the meso signals appeared at the far-upfield regions (approximately −60 ppm).[4a] As iron moves toward the porphyrin mean plane in spin-admixed complexes, the meso proton signals move *down*field while the $-CH_2$ protons move *up*field toward the diamagnetic region.[6] The chemical shifts of the $-CH_3$ protons of the ethyl substituent are also sensitive to spin states: the $S = {}^5/_2$ complex exhibits signals that are more downfield than those for the $S = {}^3/_2$ complex.[6b] However, the $-CH_3$ signals of **3** appear at 8.3, 8.1, and 6.5 ppm for core I, while for core II, the signals arise at 2.8 and 2.7 ppm. The anti-Curie temperature dependence (Figure S5), particularly for the meso proton signals, is also characteristic of admixed spin states.[6] On the basis of the above results, the spin states of the Fe(III) ions in complex **3** can be assigned as nearly high-spin and admixed intermediate spins in cores I and II, respectively, as also observed in the solid. However, it should be noted that in all previously reported μ-hydroxo complexes, the Fe centers are indistinguishable with either the admixed (for $\{[Fe(TPP)]_2(OH)\}^+$) or high-spin state (for $\{[Fe(OEP)]_2(OH)\}^+$).[2]

The small isotropic shifts in trace A (Figure 4) reflect the weak paramagnetic character of **2**, which is a consequence of strong antiferromagnetic coupling through the oxo bridge. However, μ-hydroxo complex **3** in solution produced the upfield and downfield shifts for the meso and ethylene protons, respectively (trace B), and yielded well-resolved ^{1}H NMR spectra with much larger isotropic shifts, which is indicative of relatively weaker antiferromagnetic coupling between the two iron centers. Variable-temperature magnetic susceptibility measurements were carried out for **3** in the solid state, and the plot of $\chi_M T$ versus T (Figure S6) was simulated using the expression derived from the spin Hamiltonian $\hat{H} = -2J\hat{\mathbf{S}}_1\cdot\hat{\mathbf{S}}_2 - \hat{\boldsymbol{\mu}}\cdot\mathbf{B} + D[\hat{S}_z^2 - {}^1/_3 S(S+1)]$ ($S_1 = {}^5/_2$; $S_2 = {}^3/_2$), which yielded $-J = 4.5 \pm 0.2$ cm^{-1} (see the Supporting Information for details). Thus, strong antiferromagnetic coupling in the μ-oxo dimer **2** ($-J = 126.6$ cm^{-1})[4] is attenuated to a very weak exchange interaction in the μ-hydroxo species **3**. In sharp contrast, the Fe(III) centers in the closely related μ-hydroxo complex $[Fe^{III}(OEP)]_2OH\cdot ClO_4$ are high-spin and strongly antiferromagnetically coupled with a much larger $-J$ value.[2b]

To date, the unsupported μ-hydroxo-bridged diiron(III) porphyrins available for magnetic comparison are $\{[Fe(OEP)]_2(OH)\}^+$ and $\{[Fe(TPP)]_2(OH)\}^+$, although the presence of impurities prevented an accurate determination of the exchange-coupling constant J for the former.[2a,b] The magnetostructural data for these compounds are Fe−O(H)OEP = 1.94 Å and 100 cm^{-1} < $|J_{OEP}|$ < 320 cm^{-1} for the OEP complex and Fe−O(H)TPP = 1.87 Å and $|J_{TPP}|$ < 3 cm^{-1} for the TPP complex.[2a,b] In both cases, the Fe−O distance increased in going from the μ-oxo complex to the μ-hydroxo complex, causing a sharp decrease in the coupling constant ($-J$) values. In complex **3**, the Fe−O distance also increases significantly (from 1.774 Å in μ-oxo dimer **2** to 1.916 Å in μ-hydroxo dimer **3**), leading to a large decrease in the value of $-J$ from 126.6 cm^{-1} for **2** to 4.5 cm^{-1} for **3**. However, various experimental and theoretical studies have been reported in which the correlation between the structural parameters and J in μ-oxo- and μ-hydroxo-bridged complexes have been investigated.[3a,7] The preceding analysis indicated that lengthening of the Fe−O bonds caused by protonation of the oxo bridge is the major determinant for the decrease of $-J$, while other factors such as the Fe−O−Fe bond angle and the hydroxo proton also have certain role to play.

Evidently, the hydroxo bridge provides a weaker axial ligand field than the oxo bridge. However, deformation of the ring and a weaker axial ligand field are known to play the key roles in stabilizing intermediate spin states of Fe(III) porphyrins.[6] The rings in **3** are distorted but not to equal extents, although the two cores contain exactly the same chemical entity; core II is much more distorted than core I. As a result, the Fe−N_p, Fe−O, and Fe$\cdots$$Ct_p$ distances are all different for the two Fe(III) centers, which is suitable for the stabilization of two different spins of iron with complete retention of their own spectroscopic identities in both the solid state and solution; this is unlike the behavior of all other μ-hydroxo dimers reported to date in both heme[2] and nonheme[3] systems. Experimentally, there is no proton exchange between the μ-oxo and μ-hydroxo species on the ^{1}H NMR time scale. Further work on this novel chemical system is in progress.

Acknowledgment. This paper is dedicated to Prof. Alan L. Balch on the occasion of his 70th birthday. The authors thank the Department of Science and Technology, Government of India, and CSIR, New Delhi, for financial support. S.K.G. thanks CSIR, India, for the fellowship. We are thankful to Prof. H. C. Verma and Mr. Samar Layek of the Department of Physics, IIT Kanpur, for Mössbauer data.

Supporting Information Available: Synthesis and characterization of **3**, UV−vis spectra (Figure S1), experimental and simulated ESI-MS spectrum (Figure S2), packing diagram (Figure S3), formal diagram showing the displacement of porphyrin core atoms (Figure S4), Curie plot (Figure S5), $\chi_M T$ versus T plot (Figure S6), and X-ray crystallographic data (CIF). This material is available free of charge via the Internet at http://pubs.acs.org.

References

(1) (a) Tshuva, E. Y.; Lippard, S. J. *Chem. Rev.* **2004**, *104*, 987. (b) Solomon, E. I.; Brunold, T. C.; Davis, M. I.; Kemsley, J. N.; Lee, S. K.; Lehnert, N.; Neese, F.; Skulan, A. J.; Yang, Y.-S.; Zhou, J. *Chem. Rev.* **2000**, *100*, 235.

(2) (a) Evans, D. R.; Mathur, R. S.; Heerwegh, K.; Reed, C. A.; Xie, Z. *Angew. Chem., Int. Ed. Engl.* **1997**, *36*, 1335. (b) Scheidt, W. R.; Cheng, B.; Safo, M. K.; Cukiernik, F.; Marchon, J.-C.; Debrunner, P. G. *J. Am. Chem. Soc.* **1992**, *114*, 4420. (c) Evans, D. R.; Reed, C. A. *J. Am. Chem. Soc.* **2000**, *122*, 4660.

(3) (a) Jullien, J.; Juhász, G.; Mialane, P.; Dumas, E.; Mayer, C. R.; Marrot, J.; Rivière, E.; Bominaar, E. L.; Munck, E.; Sécheresse, F. *Inorg. Chem.* **2006**, *45*, 6922. (b) Armentano, D.; De Munno, G.; Mastropietro, T. F.; Julve, M.; Lloret, F. *J. Am. Chem. Soc.* **2005**, *127*, 10778.

(4) (a) Ghosh, S. K.; Patra, R.; Rath, S. P. *Inorg. Chem.* **2010**, *49*, 3449. (b) Ghosh, S. K.; Patra, R.; Rath, S. P. *Inorg. Chem.* **2008**, *47*, 10196.

(5) Crystal data for **3**: triclinic; space group $P\bar{1}$; a = 14.4882(13) Å, b = 14.9346(13) Å, c = 20.8197(18) Å, α = 79.137(2)°, β = 71.719(2)°, γ = 86.119(2)°; V = 4200.7(6) Å^3; Z = 2; D_{calcd} = 1.417 Mg/mm^3; T = 100(2) K; no. of reflns used = 14503; θ_{max} = 25.00°; R_1 [$I > 2\sigma(I)$] = 0.053, wR_2 (all data) = 0.156; goodness of fit on F^2 = 1.039; largest diff. peak and hole; 1.832 and −1.090 e/Å^3.

(6) (a) Nakamura, M. *Coord. Chem. Rev.* **2006**, *250*, 2271. (b) Nakamura, K.; Ikezaki, A.; Ohgo, Y.; Ikeue, T.; Neya, S.; Nakamura, M. *Inorg. Chem.* **2008**, *47*, 10299. (c) Weiss, R.; Gold, A.; Terner, J. *Chem. Rev.* **2006**, *106*, 2550.

(7) (a) Chen, Z.; Xu, Z.; Zhang, L.; Yan, F.; Lin, Z. *J. Phys. Chem. A* **2001**, *105*, 9710. (b) Weihe, H.; Güdel, H. U. *J. Am. Chem. Soc.* **1997**, *119*, 6539. (c) Hart, J. R.; Rappé, A. K.; Gorun, S. M.; Upton, T. H. *Inorg. Chem.* **1992**, *31*, 5254. (d) Gorun, S. M.; Lippard, S. J. *Inorg. Chem.* **1991**, *30*, 1625.

JA107374S